

Received 4 June 2025, accepted 3 July 2025, date of publication 10 July 2025, date of current version 22 July 2025.

Digital Object Identifier 10.1109/ACCESS.2025.3587283



# **Effectiveness Evaluation of Penetration-Detection Scheme for Surgical Drill Using Thrust Force and Positional Information**

SHUNYA TAKANO<sup>®1,2</sup>, (Graduate Student Member, IEEE), TOMOYUKI SHIMONO<sup>®1,3,4</sup>, (Senior Member, IEEE), TAKUYA MATSUNAGA<sup>1</sup>, (Member, IEEE), MITSURU YAGI<sup>®5</sup>, KOUHEI OHNISHI<sup>®1,6</sup>, (Life Fellow, IEEE), MASAYA NAKAMURA<sup>®7</sup>, YUICHIRO MIMA<sup>7</sup>, KENTO YAMANOUCHI<sup>®7</sup>, AND GO IKEDA<sup>8</sup>

<sup>1</sup>Kanagawa Institute of Industrial Science and Technology, Kawasaki, Kanagawa 210-0821, Japan

Corresponding author: Shunya Takano (takano-shunya-ym@ynu.jp)

This work was supported by the Japan Agency for Medical Research and Development (AMED) under Grant 24he2202014h0103.

**ABSTRACT** The risk of spinal cord injury when cutting into the spine is a particular concern in orthopedic surgery. Surgeons must rely entirely on their haptic senses to determine bone penetration. Therefore, surgeons incur heavy burdens. Some studies have introduced penetration-detection systems using torque information. However, these method requires obtaining the characteristics of the bone before the actual cutting. Our previous study introduced an orthopedic haptic drill equipped with a penetration-detection system. This drill detects penetration by monitoring changes in the force of a linear motor. In this study, the advantage of using force over torque for penetration detection was verified through theoretical modeling and experiments. The theoretical model indicates that the thrust force reacts more sensitively than the torque at penetration. The detection methods using the force-based and torque-based methods were compared through experiments. The experimental results verified that the force-based detection method has advantages in terms of detection accuracy and detection time. The results demonstrated the efficacy of the proposed method, highlighting its potential utility in improving the accuracy and safety of orthopedic procedures.

**INDEX TERMS** Bilateral control, orthopedic surgery, penetration detection, surgical drill.

#### I. INTRODUCTION

Bone cutting and drilling are common procedures in orthopedic surgery. During spinal surgery, surgeons must exercise particular caution to cut the spine without damaging the spinal cord. Spinal cord injuries can result in serious sequelae [1], [2]. Moreover, surgeons conventionally determine bone penetration using only their haptic sense.

The associate editor coordinating the review of this manuscript and approving it for publication was Wonhee Kim.

Therefore, only significantly skilled and experienced orthopedists may conduct spinal surgery [3]. However, this is burdensome for surgeons.

Therefore, the development of a novel and safe orthopedic drill is required. Recently, studies have been conducted on new drills that automatically stop when bone penetration occurs. Osa et al. developed a drill to detect penetration by monitoring the cutting resistance of the drill bit [4], [5]. Lee and Shih developed a drill to detect penetration by monitoring the force of the load cell and the torque of the rotary

<sup>&</sup>lt;sup>2</sup>Graduate School of Engineering Science, Yokohama National University, Yokohama 240-8501, Japan

<sup>&</sup>lt;sup>3</sup>Faculty of Engineering, Yokohama National University, Yokohama 240-8501, Japan

<sup>&</sup>lt;sup>4</sup>Institute of Multidisciplinary Sciences, Yokohama National University, Yokohama 240-8501, Japan

<sup>&</sup>lt;sup>5</sup>Department of Orthopedic Surgery, School of Medicine, International University of Health and Welfare, Narita, Chiba 286-8520, Japan

<sup>&</sup>lt;sup>6</sup>Haptics Research Center, Keio University, Kawasaki, Kanagawa 233-8522, Japan

Department of Orthopedic Surgery, School of Medicine, Keio University, Shinjuku, Tokyo 160-8582, Japan

<sup>&</sup>lt;sup>8</sup>Medtronic Japan Company Ltd., Minato, Tokyo 108-0075, Japan



motor [6], [7]. Qi and Meng and Xia et al. suggested an algorithm with a wavelet transformation of force information to accurately determine the amount of penetration during drilling [8], [9]. Aziz et al. monitored changes in the thrust force and position of a robot arm for detection [10]. Dai et al. identified the drilling state using acceleration and laser displacement sensors [11], [12], [13]. Bian et al. monitored the change in thrust force using a force/torque sensor and feeding velocity of a robot arm [14]. However, these studies detected penetration using torque information or external sensors, such as force sensors or accelerometers. These external sensors typically generate a significant amount of noise. Moreover, some studies have obtained the characteristics of bone before actual cutting. However, this approach lacks adaptability, as it requires settings for each patient.

In our previous study, we developed a novel orthopedic haptic drill featuring a penetration-detection scheme [15], [16]. This drill detects penetration by monitoring changes in the force output of its linear motor. The force is estimated using positional information from the linear motor, which produces less noise than conventional force or acceleration sensors. The drill demonstrated high-accuracy penetration detection by promptly retracting the drill bit via the linear motor, thereby reducing the risk of spinal cord injury. Additionally, the drill can estimate bone characteristics in real time and adjust detection parameters during bone cutting [16], eliminating the need for manual adjustments for each patient and enhancing adaptability. Another advantage of the linear motor is its ability to immediately retract the drill tip upon penetration. In contrast, conventional detection methods only stop the drill's rotation after penetration. However, because cutting resistance suddenly drops at penetration, the drill may still advance even if the tip is no longer rotating, risking injury to sensitive tissues such as the spinal cord. Retraction of the tip using a linear motor significantly reduces this risk. Although previous studies [6], [7], and [14] have integrated the drill into robotic arms to enable tip retraction upon penetration, these systems typically have slower response times. Consequently, robotic arms may not react sufficiently quickly to prevent forward drill movement during penetration. Conversely, the fast response of linear motors allows for immediate retraction of the drill tip. Therefore, integrating a linear motor with thrust-based detection offers significant advantages in terms of detection accuracy, response speed, and safety during surgical procedures.

In this paper, the advantage of using force over torque for penetration detection was verified through theoretical modeling and experiments. The proposed penetration-detection scheme based on monitoring changes in force has advantages in terms of detection accuracy, detection time, and invasion distance after penetration. The theoretical model of thrust force and cutting torque of surgical drill was derived. The theoretical model indicates that the thrust

force reacts more sensitively than the torque at penetration, enabling faster and more accurate detection. Additionally, the comparison of detection methods using the force-based and torque-based methods were conducted by experiment. The results demonstrated the efficacy of the proposed method, highlighting its potential utility in improving the accuracy and safety of orthopedic procedures. Thus, this method can be safely introduced into conventional spinal surgical procedures.

The remainder of this manuscript is organized as follows: In Section II, the theoretical model of the thrust force and torque on the drill is described. In Section III, the structures of the orthopedic haptic drill and penetration scheme are presented. In Section IV, the theoretical model is verified using three types of wooden boards and a board-shaped artificial bone (bone board). In Section V, a comparison of the penetration schemes using a wooden board (balsa) and bone board is presented. In Section VI, the advantages of the proposed detection method and problematic issues are discussed. Finally, the conclusions are presented in Section VII.

# II. THEORETICAL MODEL OF THRUST FORCE AND TOROUE

In this section, a theoretical model of the interaction between the drilling tool and bone tissue is described. The transitions of the thrust force and cutting torque at penetration were derived using a theoretical model. According to [17], [18], [19], and [20], the thrust force  $F_t$  and cutting torque  $T_t$  of a twist drill are expressed as (1) and (2).

$$F_t = \alpha K_t \int_0^x \sin\left(\frac{\theta_t}{2}\right) \tan\left(\frac{\theta_t}{2}\right) dx \tag{1}$$

$$T_t = 2\alpha K_t \int_0^x x \tan^2\left(\frac{\theta_t}{2}\right) dx \tag{2}$$

$$\alpha = \frac{60v}{\omega} \tag{3}$$

 $\alpha$ ,  $K_t$ ,  $\theta_t$ ,  $\upsilon$ , and  $\omega$  are the feed rate, total energy per unit volume to cut the material by twist drill, convex angle of the drill tip, feeding velocity, and rotational speed, respectively. x represents the invasion length of the drill tip in the range  $0 < x \le L_t$ .  $L_t$  denotes the length of the drill-tip cone. Fig. 1(a) shows a schematic of a twist drill invading the bone. For simplicity, the effect of the chisel was not considered.

Generally, the drill bit used in orthopedic surgery has a spherical shape. Fig. 2 shows the overview of the drill bit (10BA50DC). The surface of the drill tip is coated with diamond particles, which perform bone cutting. However, these particles vary in size and shape. Thus, it is difficult to theoretically determine the edge angles and chisel effect of each particle. Accordingly, this study assumes that the particles are uniformly distributed on the spherical surface and that the convex angles are equivalent to the spherical



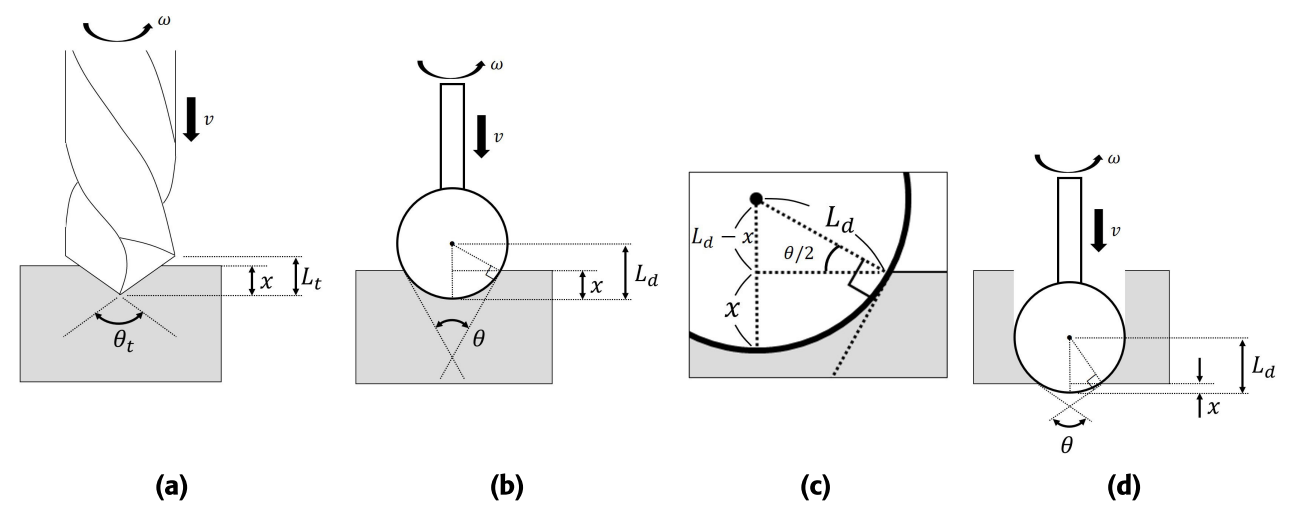


FIGURE 1. Schematics of each drill cutting the bone. (a) Twist drill invading the bone. (b) Spherical drill invading the bone. (c) Enlarged view of the spherical drill invading the bone. (d) Spherical shape drill penetrating the bone.

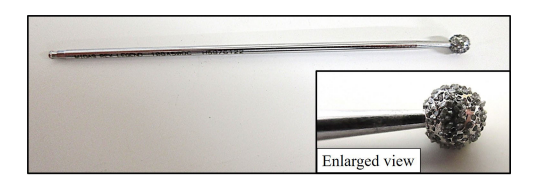


FIGURE 2. Overview of diamond bar (10BA50DC).

surface. The convex angle of the drill tip was changed according to the invasion range, as shown in Fig. 1(b), (c). In this case, the convex angle  $\theta$  of the spherical drill bit can be rewritten as (4) and (5).

$$\sin\left(\frac{\theta}{2}\right) = \frac{L_d - x}{L_d} \tag{4}$$

$$\tan\left(\frac{\theta}{2}\right) = \frac{L_d - x}{\sqrt{2L_d x - x^2}}\tag{5}$$

where  $L_d$  is the radius of the drill bit. Therefore, using (1)–(5), thrust force  $F_d$  and cutting torque  $T_d$  can be expressed as (6) and (7).

$$F_d = \alpha K_d \frac{1}{L_d} \int_0^x \frac{(L_d - x)^2}{\sqrt{2L_d x - x^2}} dx$$
 (6)

$$T_d = 2\alpha K_d \int_0^x \frac{(L_d - x)^2}{2L_d - x} dx$$
 (7)

where  $K_d$  is the total energy per unit volume to cut the material using a spherical shaped drill bit. Thus, the thrust force and cutting torque of the spherical drill bit were derived.

When the drill started penetrating the bone, as shown in Fig. 1(d), thrust force  $F_{d,p}$  and cutting torque  $T_{d,p}$  can be

derived by (8) and (9).

$$F_{d,p} = \alpha K_d \frac{1}{L_d} \int_{x}^{L_d} \frac{(L_d - x)^2}{\sqrt{2L_d x - x^2}} dx$$

$$= \alpha K_d \left\{ \frac{1}{2L_d} \sqrt{x (2L_d - x)} \cdot (x - L_d) + L_d \left( \sin^{-1} \left( \sqrt{1 - \frac{x}{2L_d}} \right) - \frac{\pi}{4} \right) \right\}$$
(8)
$$T_{d,p} = 2\alpha K_d \int_{x}^{L_d} \frac{(L_d - x)^2}{2L_d - x} dx$$

$$= \alpha K_d \left\{ x^2 + L_d^2 \left( 2 \log \left( \frac{2L_d - x}{L_d} \right) - 1 \right) \right\}$$
(9)

Subscript  $_{\rm p}$  is an initial letter of "penetration". In the experiment, 2.5 mm radius drill bit was used. Thus, the transitions in (8) and (9) at  $L_d=2.5$  mm are shown in Fig. 3(a). After the drill began to penetrate, the torque decreased gradually. In contrast, the thrust force suddenly decreased after penetration. Additionally, Fig. 3(b) shows the differential of two values. From the graph, the differential value of the thrust force shows a peak at the beginning of penetration. Thus, the thrust force reacted more sensitively than the torque when the drill started to penetrate the bone. Therefore, monitoring the differential value of the thrust force is appropriate for detecting penetration.

# III. ORTHOPEDIC HAPTIC DRILL

This section describes the structure and control method of an orthopedic haptic drill. The drill was used to verify the penetration-detection scheme.

#### A. STRUCTURE

Fig. 4(a) shows the structure of the orthopedic haptic drill, and Fig. 4(b) shows the drill schematic. The drill consisted of



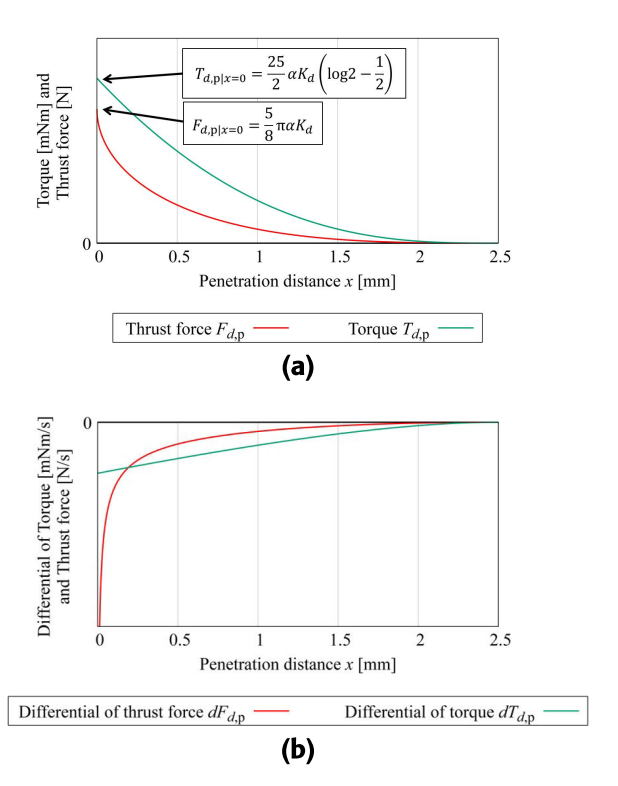
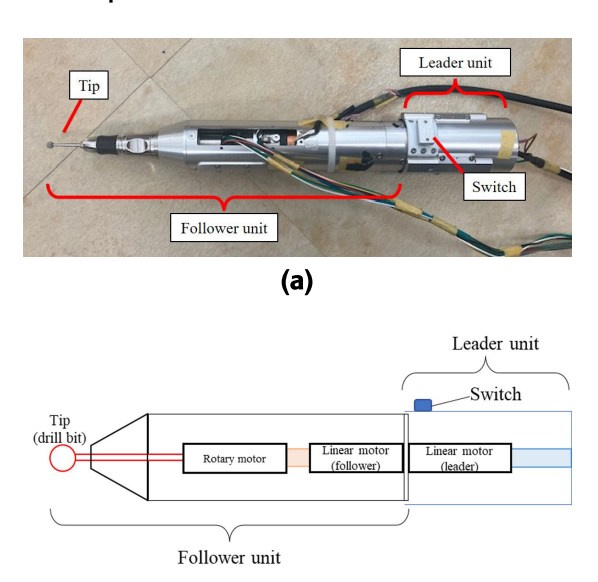


FIGURE 3. Theoretical profile of thrust force and torque after penetration. ( $L_d=2.5\,$  mm) (a) Transition of torque and thrust force. (b) Transition of differential torque and thrust force.



**FIGURE 4.** Structure of the orthopedic haptic drill. (a) General view. (b) Schematic.

(b)

two linear motors with optical encoders and one rotary motor with a rotary encoder. The linear motor was a voice-coil motor (Orbray), and the rotary motor was a brushless DC motor (Orbray BMS16-4202BOD). The specifications of each motor are listed in Table 1. Rotary and linear motors were located in the follower unit of the drill. The rotary motor was mounted on the mover of the linear motor.

**TABLE 1. Specification of motors.** 

Rotary motor	
size [mm]	$\phi 19.0 \times 115.9$
torque constant [mNm/A]	3.67
Voice-coil motor	
size [mm]	$\phi 30.0 \times 48.3$
force constant [N/A]	19.02
continuous force [N]	11.81
stroke [mm]	15

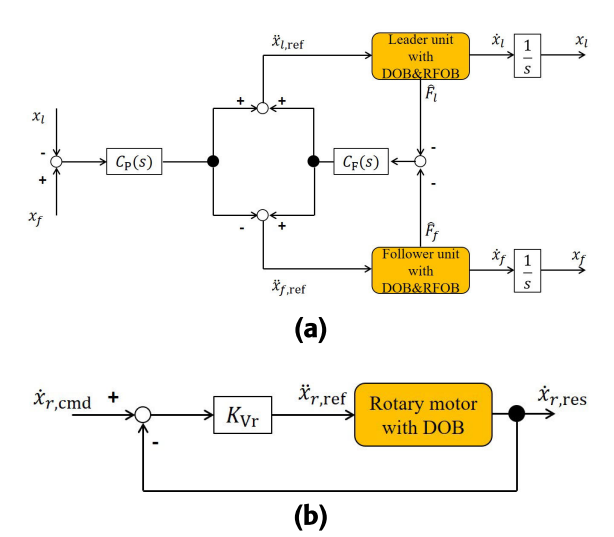


FIGURE 5. Block diagram of each control method. (a) Bilateral control. (b) Velocity control.

Therefore, the follower unit can realize the rotary and linear motions of the drill bit. The other linear motor was located in the drill leader unit. The linear motor mover was connected to the cover of the device. A switch was used to control the rotary motor attached to the cover. The surgeon handles the leader unit during surgery.

# **B. CONTROL METHOD**

The orthopedic haptic drill was controlled based on robust acceleration control using a disturbance observer (DOB) and reaction force observer (RFOB) [21], [22]. Proportional velocity control was applied to the rotary motor. Fig. 5 shows the block diagram of bilateral control and velocity control. The subscripts l and f denote the linear motors in the leader and follower units, respectively. The subscript r denotes the rotary motor in the follower unit. Additionally, subscripts r and r and r denote the command, reference, and response values, respectively. r, r, and r denote the position, velocity, and acceleration, respectively. r, r, r, and r denote the estimated reaction force, position controller, force controller, and velocity gain for rotary motor, respectively. These controllers are expressed by (10) and (11).

$$C_{P}(s) = K_{P} + K_{V} \frac{sg_{\text{diff}}}{s + g_{\text{diff}}}$$
 (10)

$$C_{\mathcal{F}}(s) = K_{\mathcal{F}} \tag{11}$$



 $K_{\rm P}$ ,  $K_{\rm V}$ ,  $K_{\rm F}$ , and  $g_{\rm diff}$  denote the positional gain, velocity gain, force gain, and cutoff frequency of pseudo-differential, respectively. Bilateral control realizes the transmission of haptic sensations between the two linear motors. Thus, the surgeon can perceive the reaction force from the drill bit while operating the leader unit.

#### C. PENETRATION-DETECTION SCHEME

In this study, we used the differential values of the position and reaction force of the linear motor on the follower unit to detect the penetration. This penetration scheme was proposed in our previous study [16]. The drill detects penetration when (12) and (13) are satisfied.

$$\dot{x}_{f,p} > 0 \tag{12}$$

$$\dot{F}_{f,p} < \dot{F}_{thd} \tag{13}$$

 $\dot{x}_{f,p}$  and  $\dot{F}_{f,p}$  are the velocity and differential value of the reaction force at the linear motor on the follower unit, respectively. Equation (12) represents the drill movement toward the cutting direction. If  $\dot{x}_{f,p} < 0$ , it indicates that the drill was retracted.  $\dot{F}_{thd}$  denotes the threshold value.  $\dot{x}_{f,p}$  and  $\dot{F}_{f,p}$  are estimated using (14) and (15).

$$\dot{x}_{f,p} = \frac{sg_p}{s + g_p} x_f \tag{14}$$

$$\dot{F}_{f,p} = \frac{sg_p}{s + g_p}\hat{F}_f \tag{15}$$

 $g_p$  is the cutoff frequency of the pseudo-differential to eliminate the high-frequency noise. Position  $x_f$  was measured using a linear encoder attached to the linear motor. The reaction force  $\hat{F}_f$  was estimated using the RFOB. The threshold value was determined using the estimated viscosity  $D_p$  as shown in (16) and (17).

$$\dot{F}_{\text{thd}} = \beta D_{\text{p}} \tag{16}$$

$$D_{\rm p} = \frac{g_{\rm p}}{s + g_{\rm p}} \cdot \frac{\hat{F}_f}{\dot{x}_{f,\rm p}} \tag{17}$$

 $\beta$  is the proportional constant and is determined experimentally based on the inertia and friction of the drill bit. The determination method is described in Section V-B. Using viscosity, the threshold value changes automatically based on the object's characteristics. For example, in the case of soft bone, the reaction force is small, and the cutting speed is high. Consequently, the viscosity  $D_p$  decreases, leading to a lower threshold  $F_{thd}$ . This allows the system to detect penetration with small changes in force. In contrast, for hard bone, the reaction force is large, and the cutting speed is low. Consequently, the threshold  $\dot{F}_{thd}$  increases. This allows the system to prevent misdetection caused by vibrations during cutting. Moreover, because the reaction force is large during cutting, the differential value of the reaction force at penetration becomes large. Thus, the system can detect penetration even at a high threshold value. Therefore, the drill can detect penetration without manually adjusting the threshold values.

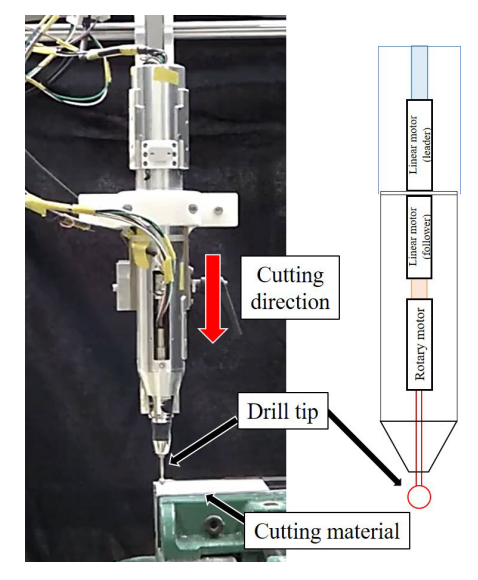


FIGURE 6. Experimental setup.

#### IV. VERIFICATION OF THEORETICAL MODEL

In this section, the theoretical model was verified using a wooden board and bone board. A comparison between the transitions of the theoretical and measured values is presented.

#### A. EXPERIMENTAL SETUP

Fig. 6 shows the experimental setup for cutting the material. The drill was fixed to an aluminum frame, and the material was fixed using a clamp. Balsa, paulownia, hinoki, and bone boards (Yasojima Proceed Standard-40) were used as the cutting objects. All wooden boards were approximately 5 mm wide, and the bone board was approximately 10 mm wide. The width of each material was measured using a caliper. The density and size of the bone board were  $560.8 \pm 56.2 \text{ kg/m}^3$ and  $100 \times 100 \times 10$  mm, respectively. A 2.5-mm radius diamond bar (Medtronic 10BA50DC) was used as the drill bit. The drill was controlled using position control. The drill cut the material at a constant speed of 0.5 mm/s. Each trial was repeated ten times. Table 2 lists the controller parameters. The sampling time was determined based on the processing speed of the controller PC. The gain and cutoff frequency were manually set to ensure stable operation of the system. The gains  $K_P$  and  $K_V$  have a relationship that makes the system stable, as shown in (18).

$$2\sqrt{K_{\rm P}} = K_{\rm V} \tag{18}$$

#### **B. EXPERIMENT RESULT**

Fig. 7 shows the experimental result of cutting each wood boards and bone board. Fig. 7(a)-(d) show the result of reaction force and Fig. 7(e)-(h) show the result of reaction torque of cutting balsa, paulownia, hinoki, and bone board, respectively. The x-axis shows the position of the drill tip, that is, the cutting depth. The offset torque after penetration is a no-load torque.



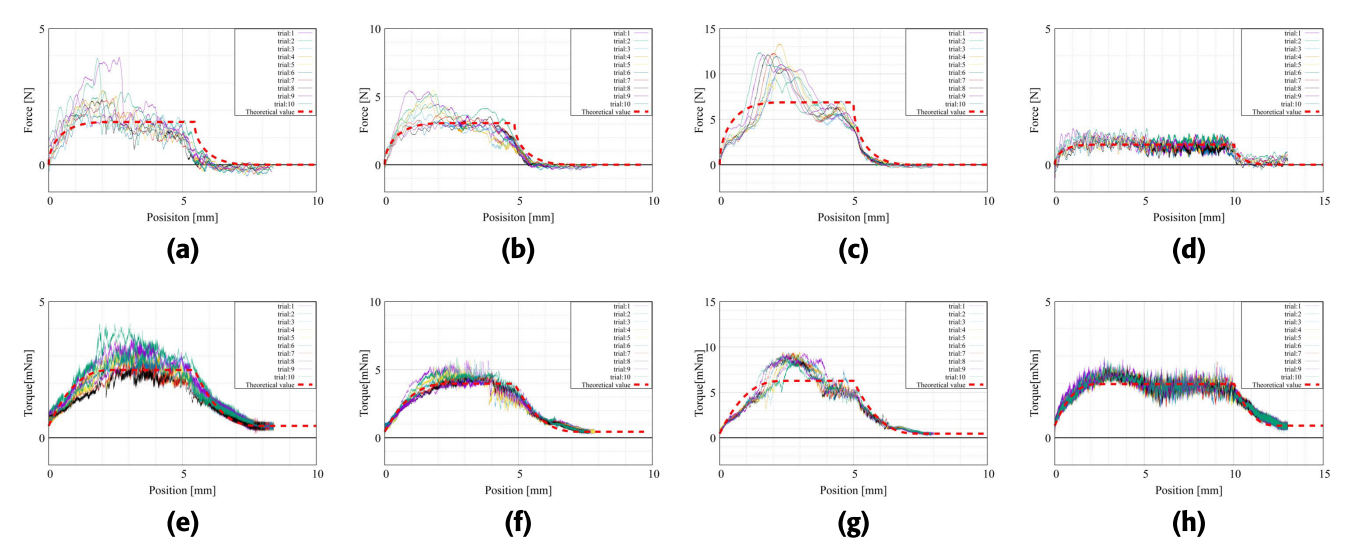


FIGURE 7. Experimental result of cutting each wood. (a) Reaction force (balsa). (b) Reaction force (paulownia). (c) Reaction force (hinoki). (d) Reaction force (bone board). (e) Reaction torque (balsa). (f) Reaction torque (paulownia). (g) Reaction torque (hinoki). (h) Reaction torque (bone board).

**TABLE 2.** Control parameters.

Parameters	Variable	
Sampling time [s]	$\Delta t$	$1.0 \times 10^{-3}$
Rotational speed [rpm]	$\omega$	30000
Radius of drill bit [mm]	$L_d$	2.5
Positional gain [s <sup>-1</sup> ]	$K_{\mathrm{P}}$	6400
Velocity gain (linear motor) [s <sup>-2</sup> ]	$K_{ m V}$	160
Velocity gain (rotary motor) [s <sup>-2</sup> ]	$K_{ m Vr}$	160
Force gain	$K_{ m F}$	1
Cutoff frequency of DOB and RFOB [rad/s]	$g_{ m dis}$	150
Cutoff frequency of pseudo-differential [rad/s]	$g_{ m diff}$	300
Cutoff frequency of pseudo-differential		
for estimate penetration signals [rad/s]	$g_{ m p}$	30

From the graph, the force and torque increased at the beginning of cutting and remained constant at approximately 2 mm. Moreover, the force and torque suddenly decreased by more than 5 and 10 mm on the wood and bone boards, respectively. This decrease represented penetration. However, the force decreased rapidly compared with the torque. For example, the force of the cutting balsa (Fig. 7(a)) was decreased at 5.4 mm and converged at 7 mm. However, the torque (Fig. 7(e)) decreases to 5.4 mm and converges to 8 mm. These trends were observed for all the materials. Therefore, the experimental results indicate that the thrust force reacts more sensitively than the torque when the drill begins to penetrate.

The red dotted line represents the theoretical value, which is approximated as all the trial data. The coefficient  $K_d$  was estimated using the least-squares method. Table 3 lists the estimated values of  $K_d$  using (8) and (9). The results show that the  $K_d$  values for balsa and paulownia are approximately the same. However,  $K_d$  estimated by the force in hinoki showed a higher value than that of the torque. In Fig. 7(c), the large thrust force were generated at approximately 1-3 mm depth. This large force is considered to be caused by the uneven stiffness of the wood grain. If the maximum force of the theoretical value is 5.5 N, which is the constant value

**TABLE 3.** Material width and estimated result of  $K_d$ .

	Balsa	Paulownia	Hinoki	Bone
				board
Material width [mm]	5.45	4.85	5.00	10.03
$K_d$ estimated by force $[\times 10^9]$	0.80	1.56	3.50	0.38
$K_d$ estimated by torque [×10 <sup>9</sup> ]	0.85	1.46	2.41	0.63

around 4 mm, the  $K_d$  is estimated to be  $2.8 \times 10^9$ . This value is close to the  $K_d$  estimated from the torque. Therefore, this difference was caused by the effect of the large thrust force. Moreover,  $K_d$  estimated by the force in the bone board shows a lower value than that of the torque. However, this difference was small. If the  $K_d$  is increased  $0.25 \times 10^9$ , the maximum force of the theoretical value is increased by only  $0.5 \, \text{N}$ . This difference can be considered the effect of friction or the modeling error of the RFOB. Thus, it can be regarded as the same value. Thus, the theoretical model was verified experimentally.

### V. COMPARISON OF PENETRATION-DETECTION SCHEME

In this section, the penetration-detection scheme was verified using a wooden board (balsa) and bone board. A comparison of the penetration-detection schemes is presented.

Two penetration schemes were used for comparison in the experiment.

- 1) The differential torque  $\dot{T}_r$  was lower than  $\dot{T}_{thd}$  [4].
- 2) The differential values of the position  $\dot{x}_{f,p}$  and reaction force  $\dot{F}_{f,p}$  of the linear motor satisfied (12) and (13).

Scheme no.1 detects penetration by monitoring the decreasing torque. The differential torque  $\dot{T}_r$  was estimated by differentiating the rotary motor torque. The torque was measured using the RFOB. Scheme 2 shows the detection of penetration by monitoring the decrease in the force.



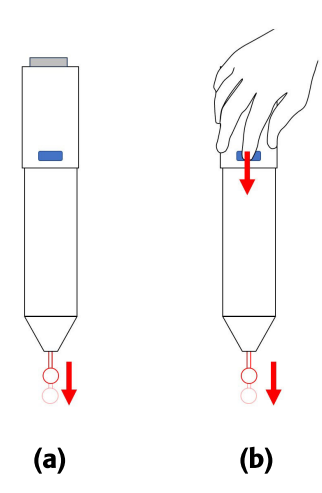


FIGURE 8. Schematics of each operation. (a) Force control. (b) Bilateral operation.

#### A. EXPERIMENTAL SETUP

The experimental setup was the same as that shown in Fig. 6. Balsa and bone boards were used as cutting materials, and a 2.5 mm radius diamond bar (Medtronic 10BA50DC) was used as the drill bit. Two types of experiments were conducted in this study.

- 1) Vertical cutting by force control (3.0 N).
- 2) Vertical cutting by bilateral control. The surgeon controlled the leader unit to cut the material.

Schematic of each operation are shown in Fig. 8. In Experiment 1, force control was applied to the follower side of the linear motor to cut the material under a constant force. In Experiment 2, bilateral control was applied to the two linear motors. The surgeon moved the leader unit to cut the material. The drill tip is retracted to the original position when the system detects penetration. The control parameters used in the experiment are listed in Table 2. Each trial was repeated ten times.

# **B.** SETTING OF THRESHOLD VALUE AND COEFFICIENT $\beta$

According to [4] and [5], the materials were cut and data were obtained to determine the parameters before the experiment. Therefore, in this study, the threshold value  $\dot{T}_{thd}$ and coefficient  $\beta$  are determined based on the characteristics of the balsa and bone board. Generally, a lower threshold value improves the detection accuracy. However, a threshold value that is too low may result in the misdetection of penetration owing to the vibrations during cutting. Therefore, the threshold value was set as low as possible within the range that avoided misdetection.

First, each material was cut using force control (3.0 N). The differential torque  $\dot{T}_r$  and coefficient  $\beta$  are measured from the beginning of cutting until penetration.  $\beta$  is estimated using (19).

$$\beta = \frac{\dot{F}_{f,p}}{D_{p}} \tag{19}$$

TABLE 4. Measurement result of threshold value.

	Bal	lsa	Bone board			
	$\dot{T}_{r,\mathrm{max}}$	$\beta_{\rm max}$	$\dot{T}_{r,\mathrm{max}}$	$\beta_{\rm max}$		
	[mNm/s]	$[\times 10^{-3}]$	[mNm/s]	$[\times 10^{-3}]$		
Average	-15.81	-2.25	-39.39	-8.43		
Standard deviation $\sigma$	3.13	0.86	6.33	4.96		
Average + $3\sigma$	-25.21	-4.84	-58.39	-23.30		
Maximum value						
of all data	-20.85	-4.03	-48.55	-19.36		

The maximum values of differential torque  $\dot{T}_{r,\text{max}}$  and coefficient  $\beta_{\text{max}}$  are recorded in each trial. These values indicate the boundary of thresholds. If the threshold values are set lower than these values, the system may cause misdetection. Cutting was performed ten times for each material. The threshold was determined based on the obtained data.

Table 4 presents the measurement results for each material. The threshold value is set as the average value  $+3\sigma$ . From the results, we determined the threshold values as (20) and (21).

$$\dot{T}_{\text{thd}} = \begin{cases}
-25.0 \text{ [mNm/s]} & \text{(balsa)} \\
-60.0 \text{ [mNm/s]} & \text{(bone board)}
\end{cases}$$
(20)

$$\beta = -25.0 \times 10^{-3} \text{ (balsa, bone board)} \tag{21}$$

Because this threshold is greater than the maximum value of all data, it allows reliable detection at penetration while avoiding misdetection of penetration. The coefficient  $\beta$  was determined based on the values obtained from the bone board, which exhibited larger values, and the same coefficient was applied to both the balsa and bone board.

#### C. EXPERIMENTAL RESULT

Table 5 lists the experimental results of cutting wood and bone board using each penetration scheme, and Table 6 shows the view of the drilled holes. "Misdetection" refers to a drill that is determined to be penetrating before the actual penetration. "No detection" refers to the drill not detecting penetration. The columns accuracy, precision, and recall represent the evaluation metrics used to assess the performance of each penetration method. Specifically, accuracy indicates how correctly the penetrations were detected, precision indicates how many of the detections identified as penetrations were actually correct, and recall indicates how many of the actual penetrations were successfully detected. These metrics are calculated using (22) - (24), where N denotes the number of trials. In particular, a low recall value implies that the system fails to detect actual penetration, which has a high risk of spinal cord injury. Therefore, it is essential that the recall value is equal to 1.

Accuracy = 
$$\frac{\text{Correct}}{N}$$
 (22)  
Precision =  $\frac{\text{Correct}}{\text{Correct+Misdetection}}$  (23)

$$Precision = \frac{Correct}{Correct + Misdetection}$$
 (23)

$$Recall = \frac{Correct}{Correct + No detection}$$
 (24)



TABLE 5. Experimental result of cutting wood and bone board.

	Data d'an annotation 1												
		Detecting penetration by					Detecting penetration using						
		linear motor's differential force.							the d	ifferential o	of rotary tor	que.	
Cutting	Cutting		Mis- No						Mis-	No			
type	material	Correct	detection	detection	Accuracy	Precision	Recall	Correct	detection	detection	Accuracy	Precision	Recall
(a) Force	Balsa	10	0	0	1.00	1.00	1.00	10	0	0	1.00	1.00	1.00
control	Bone board	10	0	0	1.00	1.00	1.00	10	0	0	1.00	1.00	1.00
(b) Bilateral	Balsa	10	0	0	1.00	1.00	1.00	6	3	1	0.60	0.67	0.86
control	Bone board	10	0	0	1.00	1.00	1.00	5	1	4	0.50	0.83	0.56
Total (A	verage)	40	0	0	1.00	1.00	1.00	31	4	5	0.78	0.89	0.86

TABLE 6. View of the hole at each experiment.

	Cutting	Detecting pe linear motor's d	enetration by ifferential force.	Detecting penetration using the differential of rotary torque.				
Cutting type	material	Front side	Back side	Front side	Back side			
(a) Force control	Balsa	8 8 8 8 8 8 8 8 8 8	460 600 600	3 3 9 9 9 8 9 9 9 9	***			
	Bone board	• • • • • • • • •	60 8 4 6 0 6 6 0 D	*******	• • • • • • • •			
(b) Bilateral control	Balsa	000000000	8	9 9 9 9 9 9 9 9 <b>9</b>	misdetection no detection			
	Bone board	999000000	39000000		misdetection no detection			

The results showed that penetration was detected in all trials using the differential force. However, detecting penetration using differential torque resulted in incorrect detection.

First, in Experiment 1, which involved force-controlled cutting, penetration was successfully detected in all trials. This is because the threshold  $\dot{T}_{thd}$  was set appropriately for each material. In contrast, in the bilateral control, incorrect detections occurred for both the balsa and bone boards. Moreover, misdetection occurred primarily at the balsa, and no detection occurred at the bone board. The reason for the misdetection in balsa is the low threshold value, which results in the misdetection of penetration due to the vibrations during cutting. Furthermore, the lack of detection in the bone board is due to the low thrust force applied by the surgeon, which results in the differential torque not exceeding the threshold at penetration.

Fig. 9 shows the results of a trial in which no detection occurred at the bone board. The red dashed line indicates the penetration point. As shown in Fig. 9(b), the reaction force was approximately 1-2 N, which is less than the 3.0 N used in the force-controlled experiment. Consequently, in Fig. 9(c), the differential torque at penetration did not exceed the threshold, resulting in a failure to detect penetration.

However, in the proposed method, penetration was correctly detected, even without adjusting the coefficient  $\beta$  across different materials with different experiments.

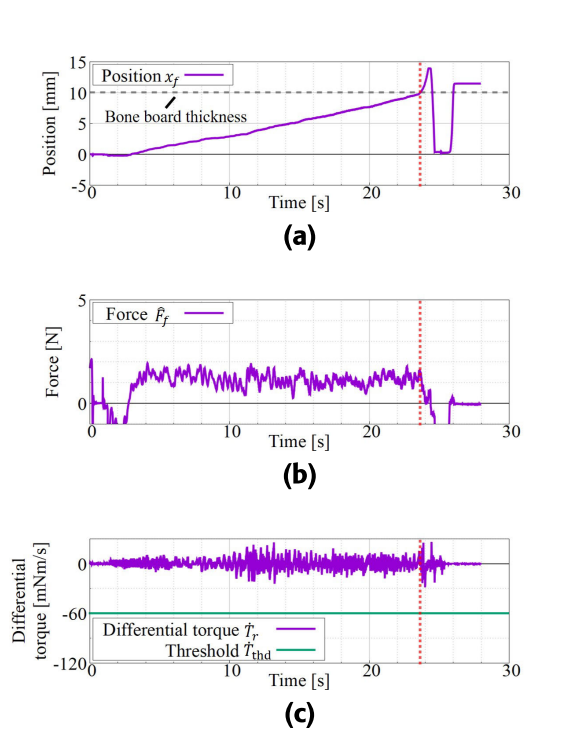


FIGURE 9. Results of cutting bone board at Experiment 2 (bilateral control) with using the differential of rotary torque. (a) Position. (b) Reaction force. (c) Differential torque.

This indicates that the proposed method achieves a higher detection accuracy.

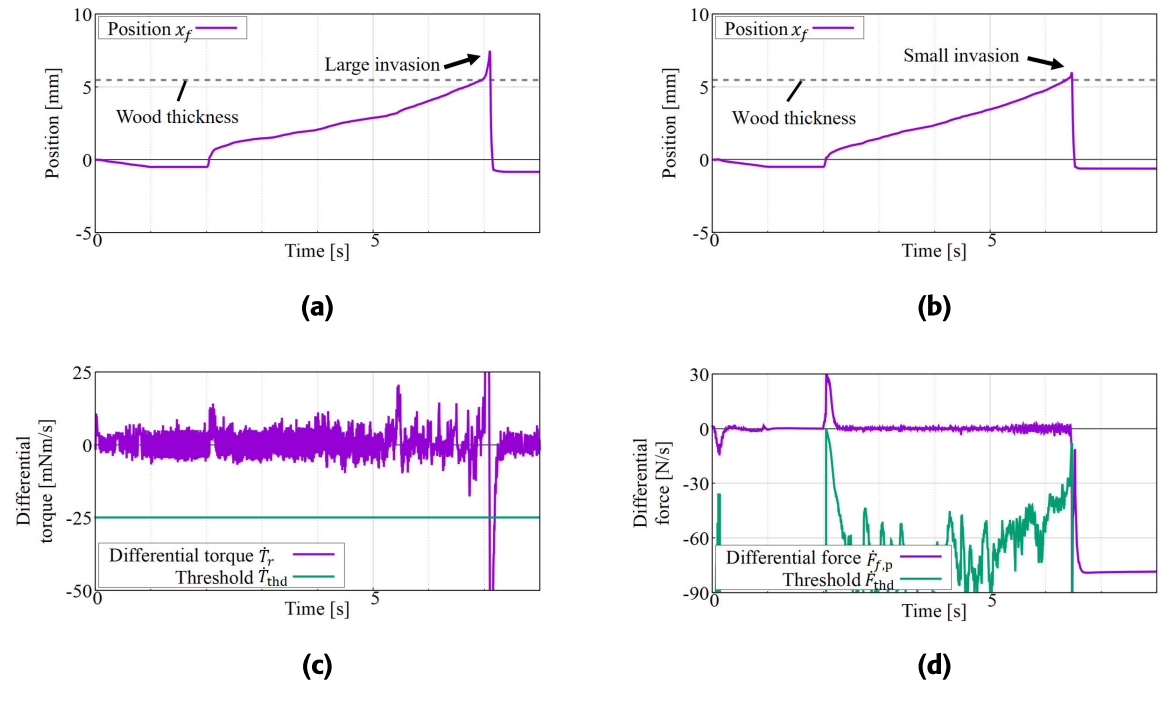


FIGURE 10. Results of cutting wood at Experiment 1 (force control). (a) Positional result for detecting penetration using the differential of rotary torque. (b) Positional result for detecting penetration using linear motor's differential force. (c) Differential torque for detecting penetration using the differential of rotary torque. (d) Differential force for detecting penetration using linear motor's differential force.

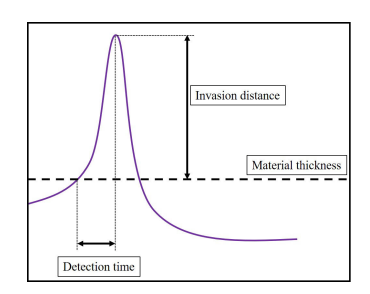
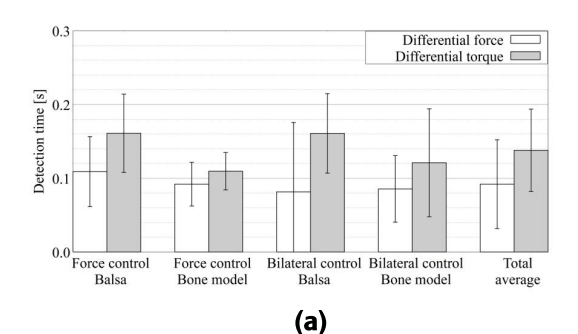


FIGURE 11. Schematic of measuring detection time and invasion distance.

Moreover, in Table 6, the size of the hole detected by the proposed method is extremely small compared with that detected by the differential torque. This indicates that the proposed method has a faster detection time and is less invasive than existing methods after penetration. Fig. 10 shows the result of cutting balsa by force control (Experiment 1). Fig. 10(a) is a result of detecting penetration by the differential torque and Fig. 10(b) is a result of detecting penetration by differential force. The dotted line represents the width of the balsa (5.45 mm). The results showed that the use of differential torque resulted in a large invasion after penetration. In contrast, the use of a differential force resulted in minimal invasion after penetration. This result verifies that the thrust force reacts more sensitively to penetration, as described by (8) and (9).

In addition, Table 7 lists the results of the detection time and invasion distance after penetration. Fig. 11 shows the



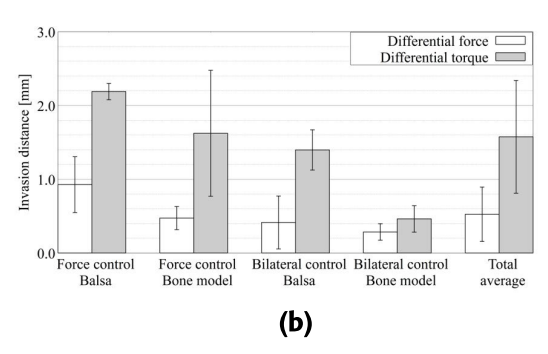


FIGURE 12. (a) Result of detection time. (b) Result of invasion distance.

measurement method of two values. Additionally, Fig. 12 shows the bar graph of Table 7. The detection time is the time taken to retract the drill bit beyond the overmaterial thickness. The invasion distance is the distance between the peak position after penetration and material thickness. The



TABLE 7. Statistic result of detection time and invasion distance.

		15:		enetration b			Detecting pe le differential		
		linear motor's differential force.  Ditection time [s] Invasion distance [mm]					n time [s]	•	istance [mm]
Cutting	Cutting	Standard			Standard		Standard		Standard
type	material	Average	deviation	Average	deviation	Average	deviation	Average	deviation
(a) Force	Balsa	0.109	0.048	0.927	0.379	0.161	0.053	2.189	0.112
control	Bone board	0.092	0.030	0.473	0.157	0.110	0.025	1.624	0.854
(b) Bilateral	Balsa	0.082	0.094	0.414	0.359	0.161	0.054	1.398	0.272
control	Bone board	0.086	0.045	0.285	0.112	0.121	0.073	0.462	0.180
Total (Average)		0.092	0.060	0.525	0.369	0.138	0.056	1.575	0.765

results showed that the proposed method exhibited faster detection and less invasion after penetration.

First, in terms of detection time, the proposed method detected penetration faster for all experiments and materials. Furthermore, the invasion distance was significantly smaller when the proposed method was used. In particular, when cutting balsa under bilateral control, the invasion distance was reduced by approximately 30%. Detection method, which uses differential torque was adjusted the threshold value for each material. In contrast, the proposed method was designed based on the bone board and did not adjust the parameters for balsa. This demonstrates the effectiveness of threshold optimization using viscosity. As shown in Fig. 10(d), the threshold value was increased and crossed with differential force at the penetration. This transition also demonstrates the effect of the proposed method. The results showed that the differential force reacted more rapidly than the differential torque, enabling faster and more accurate detection.

# VI. DISCUSSION

This study described the effectiveness of the proposed penetration-detection method by monitoring the change in thrust force. The utility of the proposed method was verified through theoretical modeling and experiments. A theoretical model of the thrust force and torque for a spherical drill was constructed. The theoretical model demonstrated that the thrust force decreased more sharply than the torque at penetration. This confirms that monitoring the differential force is more suitable for detecting penetration.

In this study, the thrust force was estimated using the positional information of the linear motor rather than using a force sensor. Therefore, less noise was generated than when using a force sensor. Moreover, in torque-based detection methods reported in previous studies, only the rotation of the drill was stopped at penetration. In contrast, the proposed method enables the retraction of the drill tip at penetration using a linear motor. This movement significantly reduces the risk of cord injury, which is the advantage of using a linear motor in the system.

In the penetration-detection experiment, the proposed method showed significant advantages in terms of detection time, accuracy, and depth of invasion after penetration. In the torque-based detection method, incorrect detections occurred during bilateral control cutting. This is due to variations in the applied force and the inconsistent feeding speed of the surgeon. In contrast, the proposed method successfully detected penetration even during manual operation. Moreover, in the torque-based detection experiment, the threshold value was adjusted for each material. However, the proposed method only adjusted the parameter for the bone board and did not change when cutting the balsa. This indicates that the proposed method has high adaptability for different bone stiffness or operations.

However, relying on thrust force information rather than torque has a disadvantage. The proposed method requires an additional linear motor, which increases the weight and size. The solution to this problem is to conduct design optimization of the motor. Currently, the voice-coil motor can generate a continuous force of 11.81 N. However, this output force is considered excessive for cutting bone. The experimental results shown in Fig. 7(d) and Fig. 10(b) show that the thrust force while cutting bone board was approximately 1-2 N. Therefore, the voice-coil motor can be replaced with a smaller and lower-output motor. In future work, we will examine the performance requirements and consider miniaturization through additional experiments. However, if the system is mounted on a robotic arm and operated remotely, the current system is applicable.

#### VII. CONCLUSION

This study describes the utility of the proposed penetrationdetection scheme. The proposed method detects penetration by monitoring changes in the linear motor force. The utility of the proposed method was verified by comparing it with other torque-based penetration schemes. First, a theoretical model of the interaction between the drilling tool and bone was developed. The thrust force and torque transitions at penetration were derived using a theoretical model. The theoretical model indicated that the thrust force reacts more sensitively than the torque at penetration. The theoretical model was verified by cutting three wooden boards and a bone board. Second, the penetration-detection scheme was conducted by cutting a wooden board (balsa) and bone board. The experimental results show that the proposed method detects penetration with higher accuracy than that using torque information. Moreover, the proposed method detected a quicker response and was less invasive after penetration.

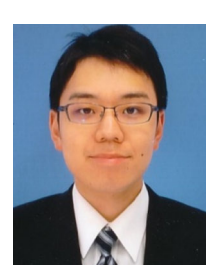


Therefore, the utility of the proposed penetration-detection scheme was verified.

#### **REFERENCES**

- [1] P. Guerin, A. B. El Fegoun, I. Obeid, O. Gille, L. Lelong, S. Luc, A. Bourghli, J. C. Cursolle, V. Pointillart, and J.-M. Vital, "Incidental durotomy during spine surgery: Incidence, management and complications. A retrospective review," *Injury*, vol. 43, no. 4, pp. 397–401, Apr. 2012.
- [2] Y. R. Rampersaud, E. R. P. Moro, M. A. Neary, K. White, S. J. Lewis, E. M. Massicotte, and M. G. Fehlings, "Intraoperative adverse events and related postoperative complications in spine surgery: Implications for enhancing patient safety founded on evidence-based protocols," *Spine*, vol. 31, no. 13, pp. 1503–1510, Jun. 2006.
- [3] Y. Imajo, T. Taguchi, K. Yone, A. Okawa, K. Otani, T. Ogata, H. Ozawa, Y. Shimada, M. Neo, and T. Iguchi, "Japanese 2011 nationwide survey on complications from spine surgery," *J. Orthopaedic Sci.*, vol. 20, no. 1, pp. 38–54, 2015.
- [4] T. Osa, C. F. Abawi, N. Sugita, H. Chikuda, S. Sugita, H. Ito, T. Moro, Y. Takatori, S. Tanaka, and M. Mitsuishi, "Autonomous penetration detection for bone cutting tool using demonstration-based learning," in *Proc. IEEE Int. Conf. Robot. Autom. (ICRA)*, May 2014, pp. 290–296.
- [5] T. Osa, C. F. Abawi, N. Sugita, H. Chikuda, S. Sugita, T. Tanaka, H. Oshima, T. Moro, S. Tanaka, and M. Mitsuishi, "Hand-held bone cutting tool with autonomous penetration detection for spinal surgery," *IEEE/ASME Trans. Mechatronics*, vol. 20, no. 6, pp. 3018–3027, Dec. 2015.
- [6] W.-Y. Lee and C.-L. Shih, "Force control and breakthrough detection of a bone drilling system," in *Proc. IEEE Int. Conf. Robot. Autom.*, May 2003, pp. 1787–1792.
- [7] W. Lee and C. Shih, "Control and breakthrough detection of a three-axis robotic bone drilling system," *Mechatronics*, vol. 16, no. 2, pp. 73–84, Ian 2006
- [8] L. Qi and M. Q.-H. Meng, "Real-time break-through detection of bone drilling based on wavelet transform for robot assisted orthopaedic surgery," in *Proc. IEEE Int. Conf. Robot. Biomimetics (ROBIO)*, Dec. 2014, pp. 601–606.
- [9] G. Xia, Z. Jiang, Y. Dai, and F. Duan, "A cutter vibration signal processing-based state monitoring method for improving operation safety of spinal automatic drilling system," *IEEE Trans. Circuits Syst. II, Exp. Briefs*, vol. 71, no. 8, pp. 4015–4019, Aug. 2024.
- [10] M. H. Aziz, M. A. Ayub, and R. Jaafar, "Real-time algorithm for detection of breakthrough bone drilling," *Proc. Eng.*, vol. 41, pp. 352–359, Jan 2012
- [11] Y. Dai, Y. Xue, and J. Zhang, "Vibration-based milling condition monitoring in robot-assisted spine surgery," *IEEE/ASME Trans. Mechatronics*, vol. 20, no. 6, pp. 3028–3039, Dec. 2015.
- [12] Y. Dai, Y. Xue, and J. Zhang, "Milling state identification based on vibration sense of a robotic surgical system," *IEEE Trans. Ind. Electron.*, vol. 63, no. 10, pp. 6184–6193, Oct. 2016.
- [13] Y. Dai, Y. Xue, and J. Zhang, "Bioinspired integration of auditory and haptic perception in bone milling surgery," *IEEE/ASME Trans. Mechatronics*, vol. 23, no. 2, pp. 614–623, Apr. 2018.
- [14] G.-B. Bian, B.-T. Wei, Z. Li, P. Ge, Z. Chen, C. Qian, J. Wang, P. Fu, and J. Zhao, "Robotic automatic drilling for craniotomy: Algorithms and in vitro animal experiments," *IEEE/ASME Trans. Mechatronics*, vol. 28, no. 6, pp. 3458–3469, Dec. 2023.
- [15] K. Yamanouchi, S. Takano, Y. Mima, T. Matsunaga, K. Ohnishi, M. Matsumoto, M. Nakamura, T. Shimono, and M. Yagi, "Validation of a surgical drill with a haptic interface in spine surgery," *Sci. Rep.*, vol. 13, no. 1, p. 598, Jan. 2023.
- [16] S. Takano, T. Shimono, T. Matsunaga, M. Yagi, K. Ohnishi, M. Nakamura, Y. Mima, K. Yamanouchi, and G. Ikeda, "Development of orthopedic haptic drill for spinal surgery with penetration detection scheme based on viscosity estimation," in *Proc. IEEE/ASME Int. Conf. Adv. Intell. Mecha*tronics (AIM), Jun. 2023, pp. 194–200.
- [17] B. Allotta, G. Giacalone, and L. Rinaldi, "A hand-held drilling tool for orthopedic surgery," *IEEE/ASME Trans. Mechatronics*, vol. 2, no. 4, pp. 218–229, Dec. 1997.
- [18] V. Colla and B. Allotta, "Wavelet-based control of penetration in a mechatronic drill for orthopaedic surgery," in *Proc. IEEE Int. Conf. Robot. Autom.*, vol. 1, May 1998, pp. 711–716.

- [19] A. Zhang, S. Zhang, C. Bian, and H. Kong, "Modified chip-evacuation force modeling and chip-clogging prediction in drilling of cortical bone," *IEEE Access*, vol. 7, pp. 180671–180683, 2019.
- [20] B. Allotta, F. Belmonte, L. Bosio, and P. Dario, "Study on a mechatronic tool for drilling in the osteosynthesis of long bones: Tool/bone interaction, modeling and experiments," *Mechatronics*, vol. 6, no. 4, pp. 447–459, Jun. 1996.
- [21] K. Ohnishi, M. Shibata, and T. Murakami, "Motion control for advanced mechatronics," *IEEE/ASME Trans. Mechatronics*, vol. 1, no. 1, pp. 56–67, Mar. 1996.
- [22] T. Murakami, F. Yu, and K. Ohnishi, "Torque sensorless control in multidegree-of-freedom manipulator," *IEEE Trans. Ind. Electron.*, vol. 40, no. 2, pp. 259–265, Apr. 1993.



SHUNYA TAKANO (Graduate Student Member, IEEE) received the B.E. and M.E. degrees in electrical and computer engineering from Yokohama National University, Yokohama, Japan, in 2015 and 2017, respectively. He is currently pursuing the Ph.D. degree since 2022. From 2019 to 2025, he had been with Kanagawa Institute of Industrial Science and Technology, Kawasaki, Japan. His research interests include haptics, motion control, and sensor devices.



**TOMOYUKI SHIMONO** (Senior Member, IEEE) received the Ph.D. degree in integrated design engineering from Keio University, Yokohama, Japan, in 2007. From 2007 to 2008, he was a Research Fellow with Japan Society for the Promotion of Science, Tokyo, Japan. From 2008 to 2009, he was a Research Associate with the Global Centers of Excellence Program, Keio University. Since 2009, he has been with the Faculty of Engineering, Yokohama National

University, Yokohama, where he is currently an Associate Professor. Since 2023, he has been in charge of the Director of the Research Center for Next-Generation Health Technology, Institute for Multidisciplinary Sciences (IMS), Yokohama National University. From 2016 to 2025, he had also been with Kanagawa Institute of Industrial Science and Technology. His research interests include haptics, motion control, medical devices, and actuators.



TAKUYA MATSUNAGA (Member, IEEE) received the B.E. degree in system design engineering and the M.E. and Ph.D. degrees in integrated design engineering from Keio University, Yokohama, in 2014, 2016, and 2017, respectively. From 2017 to 2025, he had been with Kanagawa Institute of Industrial Science and Technology, Kawasaki, Japan. His research interests include haptics, motion control, and medical robotics.



MITSURU YAGI received the M.D. and Ph.D. degrees in medical science from the School of Medicine, Keio University, Tokyo, Japan, in 1999 and 2006, respectively. Since 2023, he has been with the Department of Orthopedic Surgery, School of Medicine, International University of Health and Welfare, Chiba, Japan. He is currently a Professor and the Chair. His research interests include spinal deformities and bone metabolism.





**KOUHEI OHNISHI** (Life Fellow, IEEE) received the Ph.D. degree in electrical engineering from The University of Tokyo, Tokyo, Japan, in 1980. From 2016 to 2025, he had also been with Kanagawa Institute of Industrial Science and Technology, Kawasaki, Japan. He received the Medal of Honor with a Purple Ribbon from His Majesty, the Emperor, in 2016. He served as the President for the IEEE Industrial Electronics Society in 2008 and 2009, and the Institute of

Electrical Engineers of Japan, in 2015 and 2016.



**KENTO YAMANOUCHI** received the M.D. degree in medical science from the School of Medicine, Keio University, Tokyo, Japan, in 2015, where he is currently pursuing the Ph.D. degree. His research interests include spinal cord surgery and diseases.



MASAYA NAKAMURA received the Ph.D. degree in medical science from the School of Medicine, Keio University, Tokyo, Japan, in 1987. Since 2000, he has been with the Department of Orthopedic Surgery, Department of Medicine, School of Medicine, Keio University, Tokyo. He is currently a Professor and the Chair. His research interests include spinal cord surgery, spinal cord disease, and stem cell biology.



YUICHIRO MIMA received the Ph.D. degree in medical science from the School of Medicine, Keio University, Tokyo, Japan, in 2019. Since 2012, he has been with the Department of Orthopedic Surgery, Department of Medicine, School of Medicine, Keio University, Tokyo. His research interests include spinal cord surgery and diseases.



**GO IKEDA** received the LL.B. degree from the Faculty of Law, Keio University, Tokyo, Japan, in 1994. He has been with Medtronic Japan Company Ltd., since 2004.

. . .